Observation of an Axial-Vector State in the Study of the Decay $\psi(3686) \to \phi\eta\eta'$

M. Ablikim *et al.*[*]
(BESIII Collaboration)

(Received 14 October 2024; revised 6 March 2025; accepted 23 April 2025; published 12 May 2025)

Using $(2712.4 \pm 14.3) \times 10^6$ $\psi(3686)$ events collected with the BESIII detector at BEPCII, a partial wave analysis of the decay $\psi(3686) \to \phi\eta\eta'$ is performed with the covariant tensor approach. In addition to the established states $h_1(1900)$ and $\phi(2170)$, an axial-vector state with a mass near $2.3\ \mathrm{GeV}/c^2$ is observed for the first time. Its mass and width are measured to be $2316 \pm 9_{\mathrm{stat}} \pm 30_{\mathrm{syst}}\ \mathrm{MeV}/c^2$ and $89 \pm 15_{\mathrm{stat}} \pm 26_{\mathrm{syst}}$ MeV, respectively. The product branching fractions of $\mathcal{B}[\psi(3686) \to X(2300)\eta']\mathcal{B}[X(2300) \to \phi\eta]$ and $\mathcal{B}[\psi(3686) \to X(2300)\eta]\mathcal{B}[X(2300) \to \phi\eta']$ are determined to be $(4.8 \pm 1.3_{\mathrm{stat}} \pm 0.7_{\mathrm{syst}}) \times 10^{-6}$ and $(2.2 \pm 0.7_{\mathrm{stat}} \pm 0.7_{\mathrm{syst}}) \times 10^{-6}$, respectively. The branching fraction $\mathcal{B}[\psi(3686) \to \phi\eta\eta']$ is measured for the first time to be $(3.14 \pm 0.17_{\mathrm{stat}} \pm 0.24_{\mathrm{syst}}) \times 10^{-5}$. The first uncertainties are statistical and the second are systematic.

DOI: 10.1103/PhysRevLett.134.191901

Strangeonium ($s\bar{s}$) states can provide insight into the nonperturbative nature of QCD [1]. There are very few strangeonium resonances listed by the Particle Data Group (PDG) [2] that have been experimentally well confirmed and are widely accepted as pure $s\bar{s}$ states [3,4]. For the spectrum of axial-vector strangeonium states, only the ground axial-vector state $h_1(1380)$ [5–7] has been confirmed in PDG [2], and excited states, e.g., $h_1(2P)$ and $h_1(3P)$, have been predicted by theory [3,4,8–12] but have not been observed by experiment. And the h_1 family provides interesting possibilities to study QCD in the nonperturbative regime via the mixing mechanism, since it is sensitive to the mixing of the flavor SU(3) singlet and octet states [13,14]. The systematic search for such states, and their subsequent investigation, will supplement our knowledge about the h_1 family and improve our understanding of the strangeonium spectrum [15]. Recently, BESIII observed the 1^{+-} state, which is a candidate for the $h_1(2P)$ state [16]. However, the $h_1(3P)$ still remains unobserved by experiments.

In addition, exotic states offer a distinctive setting for investigating the dynamics of strong interactions and the confinement mechanism. Recently, the $X(6900)$, $X(6600)$, and $X(7300)$ were observed by LHCb [17], CMS [18], and ATLAS [19] collaborations. These resonances could be explained as fully charm tetraquark states, $T_{cc\bar{c}\bar{c}}$ [20–25]. Analogous to the $T_{cc\bar{c}\bar{c}}$ system, it is conceivable that stable states such as stable fully bottom tetraquark $T_{bb\bar{b}\bar{b}}$ and fully strange tetraquark $T_{ss\bar{s}\bar{s}}$ states might exist. Just like the fully heavy tetraquarks, in the fully strange tetraquarks there are no light meson exchanges, which are usually considered to be the dynamic mechanism for the formation of hadronic molecules. Theoretical calculations of the $T_{ss\bar{s}\bar{s}}$ spectrum exist, which propose the highlighted decay modes such as $\phi\eta$ and $\phi\eta'$ as crucial channels to search the $T_{ss\bar{s}\bar{s}}$ states through quark rearrangements [26–28]. The BESIII experiment has collected the world's largest J/ψ and $\psi(3686)$ datasets [29,30], and provides a unique opportunity to search $T_{ss\bar{s}\bar{s}}$ and $s\bar{s}$ states in the charmonium decays.

Based on $(2712.4 \pm 14.3) \times 10^6$ $\psi(3686)$ events accumulated by the BESIII experiment, a partial wave analysis (PWA) is performed on the decay $\psi(3686) \to \phi\eta\eta'$, where the ϕ, η, and η' mesons are reconstructed via $\phi \to K^+K^-$, $\eta \to \gamma\gamma$, and $\eta' \to \gamma\pi^+\pi^-$, respectively. This Letter presents an observation of a new axial-vector state around $2.3\ \mathrm{GeV}/c^2$ in the $\phi\eta$ and $\phi\eta'$ invariant mass spectra.

The BESIII detector records symmetric e^+e^- collisions provided by the BEPCII storage ring [31] in the center-of-mass energy range from 2.0 to 4.95 GeV, with a peak luminosity of $1 \times 10^{33}\ \mathrm{cm}^{-2}\,\mathrm{s}^{-1}$ achieved at $\sqrt{s} = 3.77$ GeV. The detailed description of the BESIII detector can be found in Ref. [32]. Simulated samples produced with GEANT4-based [33] Monte Carlo (MC) software, which includes the geometric description of the BESIII detector [34] and the detector response, are used to determine detection efficiencies and to estimate backgrounds. The simulation models the beam energy spread and initial state radiation in the e^+e^- annihilation with the generator KKMC [35,36]. An inclusive MC sample is generated to study the potential background with the production of the $\psi(3686)$ resonance simulated by the KKMC generator [35,36].

---

[*] Full author list given at the end of the Letter.

The known decay modes are modeled with EVTGEN [37,38] using branching fractions taken from the PDG [2], and the remaining unknown charmonium decays are modeled with LUNDCHARM [39,40]. Final state radiation from charged final state particles is incorporated using PHOTOS [41].

Event candidates are required to have four charged tracks with zero net charge and at least three photons. Charged tracks detected in the multilayer drift chamber are required to be within a polar angle (θ) range of $|\cos\theta| < 0.93$, where θ is defined with respect to the detector symmetry axis (z axis), and their distance of closest approach to the interaction point must be less than 10 cm along the z axis and less than 1 cm in the transverse plane. Information from the time-of-flight system and $\mathrm{d}E/\mathrm{d}x$ measurements is combined to form particle identification (PID) likelihoods for the π, K, and p hypotheses. Each track is assigned as the particle type corresponding to the hypothesis with the highest PID likelihood. Exactly two oppositely charged kaons and pions are required in each event. Photon candidates are identified using showers in the electromagnetic calorimeter (EMC). The deposited energy of each shower is more than 25 MeV in the barrel region ($|\cos\theta| < 0.80$) and more than 50 MeV in the end cap region ($0.86 < |\cos\theta| < 0.92$). To exclude showers induced by charged particles, the angle between the position of each shower in the EMC and the closest extrapolated charged track is required to be larger than 10°. To suppress electronic noise and showers unrelated to the event, the difference between the EMC time and the event start time is required to be within (0, 700) ns.

To improve the momentum resolution and to suppress background, a four-constraint (4C) kinematic fit is performed under the hypothesis of $\psi(3686) \to K^+K^-\pi^+\pi^-\gamma\gamma\gamma$ by constraining the total four-momentum of the final state particles to that of the total colliding beams. For the events with more than three photons, the combination with the smallest $\chi^2_{4\mathrm{C}}$ of the 4C fit is retained, and $\chi^2_{4\mathrm{C}} < 50$ is required. The η and η' candidates are reconstructed by minimizing $\chi^2_{\eta\eta'} = (M_{\gamma_1\gamma_2} - m_\eta)^2/\sigma_\eta^2 + (M_{\gamma_3\pi^+\pi^-} - m_{\eta'})^2/\sigma_{\eta'}^2$, where m_η and $m_{\eta'}$ are the nominal masses of the η and η' [2], $M_{\gamma_1\gamma_2}$, and $M_{\gamma_3\pi^+\pi^-}$ are the invariant masses of the $\gamma_1\gamma_2$ and $\gamma_3\pi^+\pi^-$ combinations, and σ_η and $\sigma_{\eta'}$ are their corresponding resolutions determined from the signal MC simulations, respectively. An event is accepted if η and η' candidates satisfy $|M_{\gamma_1\gamma_2} - m_\eta| < 0.025\ \mathrm{GeV}/c^2$ and $|M_{\gamma_3\pi^+\pi^-} - m_{\eta'}| < 0.020\ \mathrm{GeV}/c^2$ requirements. The ϕ candidates are selected by requiring the K^+K^- invariant mass to satisfy $|M_{K^+K^-} - m_\phi| < 0.010\ \mathrm{GeV}/c^2$, where m_ϕ is the ϕ nominal mass [2]. To improve the momentum resolution, a five-constraint kinematic fit is performed with the extra constraint in which the invariant mass of two photons originating from η is constrained to m_η, and the resulting kinematic variables are used for further analysis.

To suppress contamination from $\psi(3686) \to K^+K^-\pi^+\pi^-\gamma\gamma\gamma\gamma$ and $\psi(3686) \to K^+K^-\pi^+\pi^-\gamma\gamma$ decays, two additional 4C kinematic fits under the hypotheses of $\psi(3686) \to K^+K^-\pi^+\pi^-\gamma\gamma\gamma\gamma$ and $\psi(3686) \to K^+K^-\pi^+\pi^-\gamma\gamma$ are performed. The events are discarded if the corresponding $\chi^2_{4\mathrm{C}}$ is less than the $\chi^2_{4\mathrm{C}}$ for the signal hypothesis. To reject background from $\psi(3686) \to \gamma\chi_{cJ}$ with the subsequent decay $\chi_{cJ} \to K^+K^-\pi^+\pi^-\gamma\gamma$ and background from $\psi(3686) \to \pi^+\pi^-J/\psi$ with the decay $J/\psi \to \gamma\gamma\gamma K^+K^-$, the requirements $|M_{K^+K^-\pi^+\pi^-\gamma\gamma} - M_{\chi_{cJ}}| > 0.010\ \mathrm{GeV}/c^2$ and $|M_{\gamma\gamma\gamma K^+K^-} - M_{J/\psi}| > 0.030\ \mathrm{GeV}/c^2$ are applied. The requirement $|M_{\gamma\pi^+\pi^-K^+K^-} - M_{J/\psi}| > 0.030\ \mathrm{GeV}/c^2$ is used to remove the background of $\psi(3686) \to \eta J/\psi$ with $J/\psi \to \gamma\pi^+\pi^-K^+K^-$.

After imposing all the selection criteria, the distribution of $M_{K^+K^-}$ versus $M_{\gamma\pi^+\pi^-}$ is illustrated in Fig. 1(a). A clear accumulation of candidate events for the decay $\psi(3686) \to \phi\eta\eta'$ is observed. Figures 1(b) and 1(c) show the $M_{\gamma\pi^+\pi^-}$ and $M_{K^+K^-}$ distributions. Potential backgrounds are studied using an inclusive MC sample of 2.747×10^9 $\psi(3686)$ events. No significant peaking background is observed in the signal region. Therefore, the two-dimensional sideband method is used to estimate the combinatorial backgrounds by combining the background events in the ϕ sideband region ($1.05\ \mathrm{GeV}/c^2 < M_{K^+K^-} < 1.07\ \mathrm{GeV}/c^2$) and the

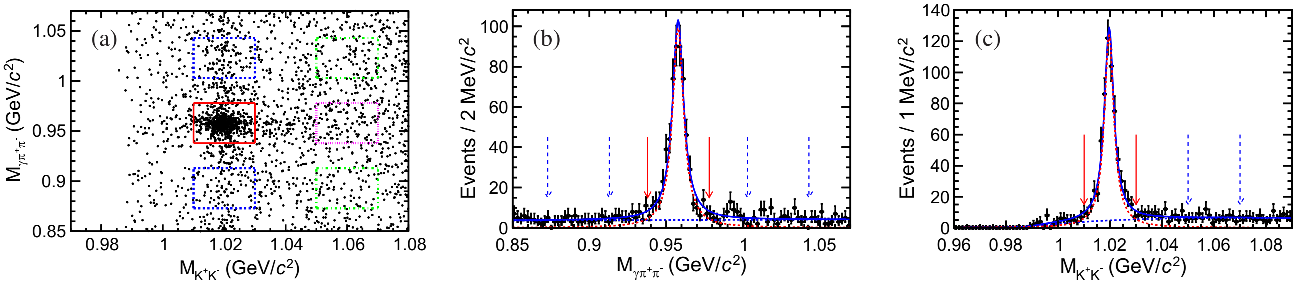

FIG. 1. (a) Distribution of $M(K^+K^-)$ versus $M(\gamma\pi^+\pi^-)$, where the red solid box shows the signal region and the dotted and dashed boxes are the sideband regions for the ϕ and η'. (b) Distribution of $M(\gamma\pi^+\pi^-)$ within the ϕ signal region. (c) Distribution of $M(K^+K^-)$ within the η' signal region. (d) Dalitz plot of $M^2(\phi\eta)$ versus $M^2(\phi\eta')$ in the signal regions. The solid arrows show the signal regions and the dashed arrows show the sideband regions.

η' sideband region ($0.045\ \mathrm{GeV}/c^2 < |M_{\gamma\pi^+\pi^-} - M_{\eta'}| < 0.085\ \mathrm{GeV}/c^2$), which are illustrated by the colored dashed boxes in Fig. 1(a). The normalization factors for the event yields in the two sideband regions are obtained from the fits to the invariant mass spectra of $M_{\gamma\pi^+\pi^-}$ and $M_{K^+K^-}$. The signal shapes are taken directly from signal MC simulation. The backgrounds are described with a first-order Chebychev polynomial function for $M_{\gamma\pi^+\pi^-}$ and an ARGUS function [42] for $M_{K^+K^-}$. The selected data sample contains a total of 597 ± 25 candidate events including 94 ± 10 background events estimated from the sideband region and normalized to the signal region.

To investigate the continuum background contribution from nonresonant e^+e^- annihilation ($e^+e^- \to \phi\eta\eta'$), the same selection criteria and sideband definition are applied in the analysis of the data sample taken at a center-of-mass energy of 3.773 GeV corresponding to an integrated luminosity of 2.93 fb^{-1}. The number of continuum background events is extracted and normalized to the $\psi(3686)$ data, taking into account the integrated luminosity and energy-dependent cross section of the continuum processes [29,30,43], and is estimated to be 23 ± 7 events. By subtracting sideband and continuum background components from the total number of candidate events, the signal yield is determined to be $N_{\mathrm{sig}} = 480 \pm 26$, where the uncertainty is statistical.

Figure 2 shows the Dalitz plot for these events in the signal regions. Figure 3 shows the projections of $\phi\eta$, $\phi\eta'$, and $\eta\eta'$ invariant mass ($M_{\phi\eta}$, $M_{\phi\eta'}$, and $M_{\eta\eta'}$) and the corresponding angular distributions, after background subtraction, for the candidate events. A structure with a mass around 2.3 GeV/c^2 in the $M_{\phi\eta}$ and $M_{\phi\eta'}$ distributions is clearly observed. To determine the properties of the newly observed structure, a PWA based on the GPUPWA framework [44] is performed. Quasi-two-body decay amplitudes in the three sequential decay processes—$\psi(3686) \to \phi X$ with $X \to \eta\eta'$, $\psi(3686) \to \eta X$ with $X \to \phi\eta'$, and $\psi(3686) \to \eta' X$ with $X \to \phi\eta$—are constructed using the covariant tensor amplitudes described in Ref. [45]. The intermediate states are parametrized with a relativistic Breit-Wigner (BW) function with mass-dependent width. Parameters of the known intermediate states are fixed to the PDG average values. The complex coefficients of the amplitudes (relative magnitudes and phases) and resonance parameters (mass and width) are determined by an unbinned maximum likelihood fit. The probability of observing N events in the data sample is

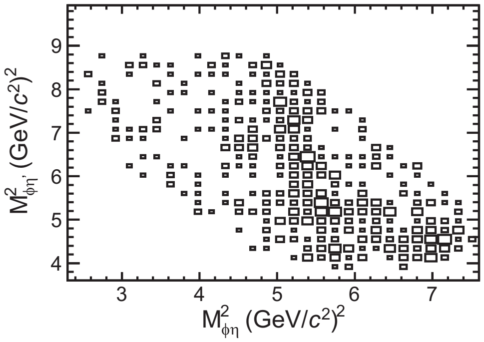

FIG. 2. Dalitz plot of $M^2(\phi\eta)$ versus $M^2(\phi\eta')$ in the signal regions.

$$S(\xi) = -\ln\mathcal{L} = -\sum_{i=1}^{N} \ln\left(\frac{|M(\xi_i)|^2 \varepsilon(\xi_i)}{\sigma'}\right), \qquad (1)$$

where ξ_i stands for all kinematic variables in the ith event, $\varepsilon(\xi_i)$ is the detection efficiency, and $M(\xi_i) = \sum A(\xi_i)$ is the matrix element describing the decay processes from $\psi(3686)$ to the final state $\phi\eta\eta'$. In addition, $A(\xi_i)$ is the amplitude of the corresponding intermediate resonance and $\sigma' = \int d\Phi |M(\xi)|^2 \varepsilon(\xi)$ is the normalization integral. The background is taken into account by subtracting normalized sideband and continuum events from the total log likelihood value. The free parameters are optimized using MINUIT [46].

In the fit procedure, all intermediate states reported by the PDG and which conserve quantum numbers J^{PC} are considered, shown in Supplemental Material [47]. Specifically, for the $\eta\eta'$ systems, resonances with $J^{PC} = 0^{++}, 1^{-+}, 2^{++}$, and 4^{++} are included, while for the $\phi\eta(\eta')$ systems, resonances with $J^{PC} = 1^{--}, 1^{+-}, 2^{--}$, and 3^{--} are taken into account. Coherent nonresonant components are also taken into account by including very broad intermediate states in the fit. The fitting procedure starts with a baseline solution incorporating phase space (PHSP) and the established $\phi(2170)$ and $h_1(1900)$ states, progressively adding all other possible intermediate resonances one by one. The statistical significance of each resonance is evaluated by examining the change in the log likelihood value and the number of free parameters in the fit with and without the resonance included, listed in Supplemental Material [47]. All components with a statistical significance greater than 5σ are added to the baseline solution. After that, all the removed components are tested again to make sure that they still do not satisfy the 5σ requirement. It is found that the resulting baseline solution does not adequately describe the structure around 2.3 GeV/c^2 in the $\phi\eta$ and $\phi\eta'$ invariant mass spectra, so an additional resonance is added to the fit. To investigate the J^{PC} of the additional resonance, different J^{PC} combinations are tested and the 1^{+-} combination is found to produce the largest change of the log likelihood value. The final set of amplitudes therefore contains a significant contribution from an axial-vector state with $J^{PC} = 1^{+-}$, denoted as $X(2300)$. The Argand diagram is shown in Supplemental Material [47]. Possible J^{PC} assignments of the structure, i.e., 1^{--}, 2^{--}, 3^{--}, and 2^{+-}, were tested. However, none of these assignments exceeded a statistical significance of 5σ, leading us to discard these

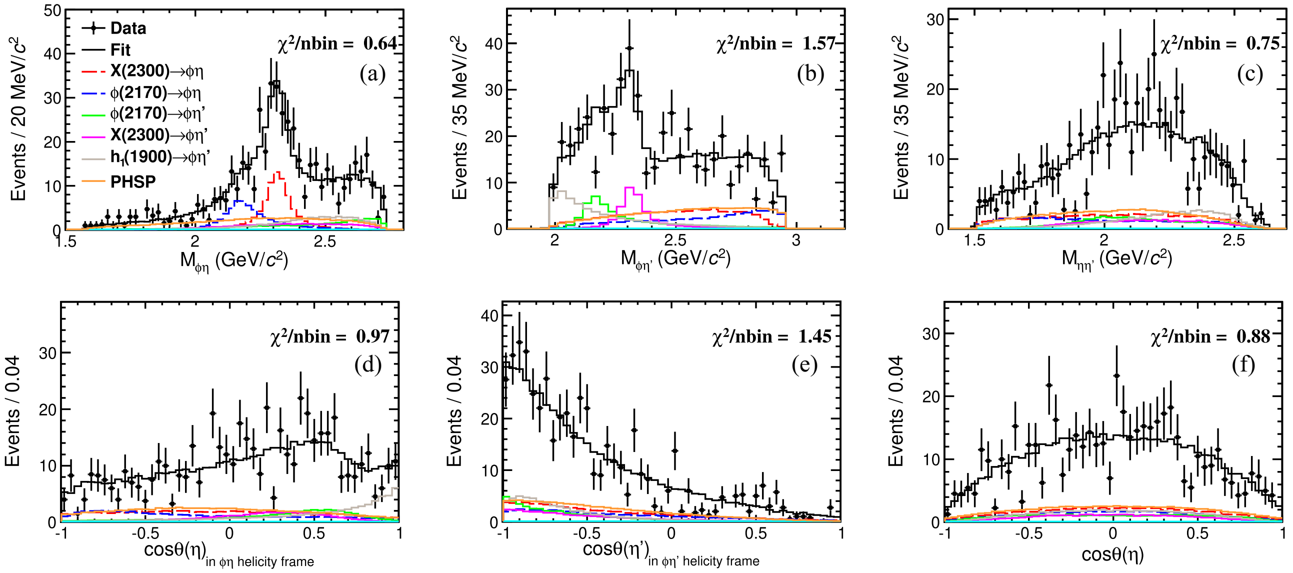

FIG. 3. Background-subtracted data (black dots) and PWA fit projections (black lines) for the invariant mass distributions of (a) $\phi\eta$, (b) $\phi\eta'$, and (c) $\eta\eta'$, and for the angular distributions of (d) $\cos\theta$ of the η in the $\phi\eta$ helicity frame, (e) $\cos\theta$ of the η' in the $\phi\eta'$ helicity frame, and (f) $\cos\theta$ of the η in the center-of-mass rest frame.

alternatives. Its significance is 9.6σ and the corresponding mass and width are determined to be 2316 ± 9 MeV$/c^2$ and 89 ± 15 MeV by a scan of the log likelihood value. The fit fractions for each component and the interference fractions between two components are listed in Supplemental Material [47].

The PWA results with the baseline set of amplitudes, including the masses and widths of the resonances, the product branching fraction of each component, and the statistical significances are summarized in Table I.

Figure 3 shows the invariant mass distributions of $\phi\eta$, $\phi\eta'$, and $\eta\eta'$ for the data, the PWA fit projections, and the angular distribution of $\cos\theta(\eta)$, $\cos\theta(\eta')$, and $\cos\theta(\phi)$ in the corresponding helicity frame.

The signal efficiency of $\psi(3686) \to \phi\eta\eta'$ is determined to be 9.88% using the MC sample weighted according to the PWA result. The total branching fraction of $\psi(3686) \to \phi\eta\eta'$ is calculated to be $(3.14 \pm 0.17_{\mathrm{stat}} \pm 0.24_{\mathrm{syst}}) \times 10^{-5}$, where the first uncertainty is statistical and the second is systematic.

Sources of systematic uncertainties are considered in two categories, non-PWA-related and PWA-related systematics. The first category includes the uncertainties of photon detection efficiency (1.0% per photon) [50], multilayer drift chamber tracking efficiency (1.0% per charged track) [51], PID efficiency (1.0% per charged track) [52], 4C kinematic fit (1.3%), ϕ, η, and η' mass windows (1.5%, 0.2%, 0.6%), quoted branching fractions (1.8%) [2], total number of $\psi(3686)$ events (0.5%), MC statistics (0.3%), and continuum background (1.6%). The uncertainty related to the 4C kinematic fit is estimated by correcting the helix parameters of the simulated charged tracks to match the resolution in the data [53]. The difference between the signal efficiencies with and without correction is regarded as the systematic uncertainty. The systematic uncertainties from the mass resolution are estimated by fitting the mass spectrum with the MC shape convolved with a fixed-parameter Gaussian function, where the fixed parameters are extracted from control samples of $\psi(3686) \to \phi\pi^+\pi^-$ and $\psi(3686) \to \omega\eta\eta'$. The resulting changes on the signal

TABLE I. The obtained masses, widths, product branching fractions, and statistical significances (Sig.) for the $\psi(3686)$ decay and the subsequent intermediate state decay, where the first uncertainties are statistical, and the second systematic. The term "N/A" denotes unavailability.

Process	M (MeV$/c^2$)	Γ (MeV)	$\mathcal{B}$ (10^{-6})	Sig.
$h_1(1900)\eta$ [16]	1911	149	$3.8 \pm 1.4 \pm 1.5$	5.3σ
$\phi(2170)\eta$ [2]	2162	100	$3.3 \pm 1.4 \pm 1.2$	5.1σ
$\phi(2170)\eta'$ [2]			$3.8 \pm 0.9 \pm 0.5$	6.0σ
$X(2300)\eta$	$2316 \pm 9 \pm 30$	$89 \pm 15 \pm 26$	$2.2 \pm 0.7 \pm 0.7$	5.6σ
$X(2300)\eta'$			$4.8 \pm 1.3 \pm 0.7$	9.6σ
PHSP	N/A	N/A	$6.1 \pm 2.3 \pm 1.8$	5.2σ

yields are taken as the systematic uncertainty. The second category, which includes the uncertainties from the resonance description, resonance parameters, extra resonances, the Blatt Weisskopf barrier factor [54,55] that is included in the PWA decay amplitudes, and background uncertainty, which all arise from the PWA fit procedure, affects the measurements of both the branching fraction and resonance parameters. The statistical significance of $X(2300)$ is recalculated in every variation shown in Supplemental Material [47]. To estimate these uncertainties, alternative fits with different scenarios are performed, and the resulting changes on the branching fractions and the resonance parameters are taken as the systematic errors. Uncertainties from the BW parametrization are estimated by replacing the mass-dependent-width BW with the constant width. Uncertainties from the resonance parameters are estimated by fitting with masses and widths fixed to the values randomly generated from Gaussian distributions with their uncertainties taken from the PDG and the standard deviation of the results is taken as the uncertainty. The uncertainties related to extra resonances are estimated by adding known resonances with significances greater than 3σ and an additional possible structure around $2.6\ \mathrm{GeV}/c^2$ with $J^{PC} = 1^{+-}$. The largest change from the nominal PWA fit is taken as the uncertainty. Uncertainties due to the barrier factor [54,55] are estimated by varying the radius of the centrifugal barrier from 0.7 to 1.0 fm. The uncertainty associated with the background description is estimated by using different sideband regions, and changing the background level by varying the sideband normalization factors by one standard deviation. The $X(2300)$ remains larger than 5σ in $\phi\eta'$ and 9σ in $\phi\eta$. Assuming that all the sources of uncertainties are independent, the total uncertainties are estimated as the quadratic sum of the above individual values.

In summary, using $(2712.4 \pm 14.3) \times 10^6$ $\psi(3686)$ events collected by the BESIII detector, a PWA of the decay $\psi(3686) \to \phi\eta\eta'$ is performed. The analysis results in the first observation of an axial-vector state around $2.3\ \mathrm{GeV}/c^2$. Its mass and width are measured to be $2316 \pm 9_{\mathrm{stat}} \pm 30_{\mathrm{syst}}\ \mathrm{MeV}/c^2$ and $89 \pm 15_{\mathrm{stat}} \pm 26_{\mathrm{syst}}$ MeV, respectively. The product branching fractions of $\mathcal{B}[\psi(3686) \to X(2300)\eta']\mathcal{B}[X(2300) \to \phi\eta]$, and $\mathcal{B}[\psi(3686) \to X(2300)\eta]\mathcal{B}[X(2300) \to \phi\eta']$ are determined to be $(4.8 \pm 1.3_{\mathrm{stat}} \pm 0.7_{\mathrm{syst}}) \times 10^{-6}$ and $(2.2 \pm 0.7_{\mathrm{stat}} \pm 0.7_{\mathrm{syst}}) \times 10^{-6}$, respectively, where the first uncertainty is statistical and the second is systematic. The branching fraction $\mathcal{B}[\psi(3686) \to \phi\eta\eta']$ is measured for the first time to be $(3.14 \pm 0.17_{\mathrm{stat}} \pm 0.24_{\mathrm{syst}}) \times 10^{-5}$.

Theoretical predictions concerning parameters of the axial-vector $s\bar{s}$ state $h_1(3\mathrm{P})$ and the 1S wave multiplets $T_{(ss\bar{s}\bar{s})1^{+-}}$ are presented in Table II. For the $h_1(3\mathrm{P})$ hypothesis, the mass of the observed resonance is inconsistent with that of theoretical calculations. In the case of the $T_{(ss\bar{s}\bar{s})1^{+-}}$ hypothesis, the limited availability of theoretical predictions cannot exclude this possibility. To clarify the nature of the $X(2300)$, further efforts are required from both theoretical and experimental perspectives. The $X(2300)$ observed in this Letter provides important insights into the axial-vector strangeonium spectrum and $T_{ss\bar{s}\bar{s}}$.

TABLE II. Comparison of experimental measurements and theoretical predictions for the mass and width of the $h_1(3P)$ and $T_{ss\bar{s}\bar{s}}$ resonances. The term “N/A” denotes unavailability.

Resonance	M (MeV/c^2)	Γ (MeV)
$h_1(3P)$	2435 [4]	269 [4]
$h_1(3P)$	2449 [8]	N/A
$h_1(3P)$	2100 [12,15]	N/A
$h_1(3P)$	2490 [9]	N/A
$h_1(3P)$	2398 [10]	N/A
$h_1(3P)$	2495.51 ± 1.46 [11]	N/A
$h_1(4P)$	2340 [12,15]	N/A
$T_{(ss\bar{s}\bar{s})1^{+-}}$	2323 [26]	N/A
$T_{(ss\bar{s}\bar{s})1^{+-}}$	1960 [27]	N/A
$T_{(ss\bar{s}\bar{s})1^{+-}}$	2000^{+100}_{-90} [28]	N/A
This Letter	$2316 \pm 9 \pm 30$	$89 \pm 15 \pm 26$

Acknowledgments—The authors would like to thank Professor Xian-Hui Zhong and Professor Xiang Liu for their valuable theoretical discussions. The BESIII Collaboration thanks the staff of BEPCII, the IHEP computing center, and the supercomputing center of USTC for their strong support. This work is supported in part by National Key R&D Program of China under Contracts No. 2023YFA1609400, No. 2020YFA0406400, No. 2020YFA0406300; National Natural Science Foundation of China (NSFC) under Contracts No. 11635010, No. 11735014, No. 11835012, No. 11935015, No. 11935016, No. 11935018, No. 11961141012, No. 12022510, No. 12025502, No. 12035009, No. 12035013, No. 12192260, No. 12192261, No. 12192262, No. 12192263, No. 12192264, No. 12192265, No. 11335008, No. 11625523, No. 12035013, No. 11705192, No. 11950410506, No. 12061131003, No. 12105276, No. 12122509, No. 12225509, No. 12205255, No. 12235017; The Chinese Academy of Sciences (CAS) Large-Scale Scientific Facility Program; Joint Large-Scale Scientific Facility Funds of the NSFC and CAS under Contracts No. U1832207, No. U1732263, No. U1832103, No. U2032111, No. U2032105; The CAS Center for Excellence in Particle Physics (CCEPP); 100 Talents Program of CAS; CAS Project for Young Scientists in Basic Research YSBR-101; The Institute of Nuclear and Particle Physics (INPAC) and Shanghai Key Laboratory for Particle Physics and Cosmology; ERC under Contract No. 758462; European Union's Horizon 2020 research and innovation programme under Marie

Sklodowska-Curie grant agreement under Contract No. 894790; German Research Foundation DFG under Contract No. 443159800, Collaborative Research Center CRC 1044, GRK 2149; Istituto Nazionale di Fisica Nucleare, Italy; Ministry of Development of Turkey under Contract No. DPT2006K-120470; National Science and Technology fund; National Science Research and Innovation Fund (NSRF) via the Program Management Unit for Human Resources and Institutional Development, Research and Innovation under Contract No. B16F640076; Olle Engkvist Foundation under Contract No. 200-0605; STFC (United Kingdom); Suranaree University of Technology (SUT), Thailand Science Research and Innovation (TSRI), and National Science Research and Innovation Fund (NSRF) under Contract No. 160355; The Royal Society, UK under Contract No. DH140054, No. DH160214; The Swedish Research Council; U.S. Department of Energy under Contract No. DE-FG02-05ER41374.

[1] S. Godfrey and N. Isgur, Phys. Rev. D **32**, 189 (1985).
[2] R. L. Workman *et al.* (Particle Data Group), Prog. Theor. Exp. Phys. **2022**, 083C01 (2022).
[3] T. Barnes, N. Black, and P. R. Page, Phys. Rev. D **68**, 054014 (2003).
[4] Q. Li, L. C. Gui, M. S. Liu, Q. F. Lü, and X. H. Zhong, Chin. Phys. C **45**, 023116 (2021).
[5] A. Abele *et al.* (Crystal Barrel Collaboration), Phys. Lett. B **415**, 280 (1997).
[6] M. Ablikim *et al.* (BESIII Collaboration), Phys. Rev. D **91**, 112008 (2015).
[7] M. Ablikim *et al.* (BESIII Collaboration), Phys. Rev. D **98**, 072005 (2018).
[8] L. Y. Xiao, X. Z. Weng, X. H. Zhong, and S. L. Zhu, Chin. Phys. C **43**, 113105 (2019).
[9] S. Ishida and K. Yamada, Phys. Rev. D **35**, 265 (1987).
[10] D. Ebert, R. N. Faustov, and V. O. Galkin, Phys. Rev. D **79**, 114029 (2009).
[11] J. Oudichhya, K. Gandhi, and A. K. Rai, Phys. Rev. D **108**, 014034 (2023).
[12] L. M. Wang, J. Z. Wang, S. Q. Luo, J. He, and X. Liu, Phys. Rev. D **101**, 034021 (2020).
[13] H. Y. Cheng, Phys. Lett. B **707**, 116 (2012).
[14] D. M. Li, B. Ma, and H. Yu, Eur. Phys. J. A **26**, 141 (2005).
[15] K. Chen, C. Q. Pang, X. Liu, and T. Matsuki, Phys. Rev. D **91**, 074025 (2015).
[16] M. Ablikim *et al.* (BESIII Collaboration), Phys. Rev. D **110**, 112014 (2024).
[17] R. Aaij *et al.* (LHCb Collaboration), Sci. Bull. **65**, 1983 (2020).
[18] A. Hayrapetyan *et al.* (CMS Collaboration), Phys. Rev. Lett. **132**, 111901 (2024).
[19] G. Aad *et al.* (ATLAS Collaboration), Phys. Rev. Lett. **131**, 151902 (2023).
[20] V. O. Galkin and E. M. Savchenko, Eur. Phys. J. A **60**, 96 (2024).
[21] S. S. Agaev, K. Azizi, B. Barsbay, and H. Sundu, Nucl. Phys. **A1041**, 122768 (2024).
[22] J. Z. wang, D. Y. Chen, X. Liu, and T. Matsuki, Phys. Rev. D **103**, 071503 (2021).
[23] M. A. Bedolla, J. Ferretti, C. D. Roberts, and E. Santopinto, Eur. Phys. J. C **80**, 1004 (2020).
[24] M. S. liu, F. X. Liu, X. H. Zhong, and Q. Zhao, Phys. Rev. D **109**, 076017 (2024).
[25] J. F. Giron and R. F. Lebed, Phys. Rev. D **102**, 074003 (2020).
[26] F. X. Liu, M. S. Liu, Ming-Sheng, X. H. Zhong, and Q. Zhao, Phys. Rev. D **103**, 016016 (2021).
[27] Q. F. Lü, K. L. Wang, and Y. B. Dong, Chin. Phys. C **44**, 024101 (2020).
[28] E. L. Cui, H. M. Yang, H. X. Chen, W. Chen, and C. P. Shen, Eur. Phys. J. C **79**, 232 (2019).
[29] M. Ablikim *et al.* (BESIII Collaboration), Chin. Phys. C **48**, 093001 (2024).
[30] M. Ablikim *et al.* (BESIII Collaboration), Chin. Phys. C **46**, 074001 (2022).
[31] C. H. Yu *et al.*, in *Proceedings of IPAC2016, Busan, Korea* (JACoW, Busan, 2016).
[32] M. Ablikim *et al.* (BESIII Collaboration), Nucl. Instrum. Methods Phys. Res., Sect. A **614**, 345 (2010).
[33] S. Agostinelli *et al.* (GEANT4 Collaboration), Nucl. Instrum. Methods Phys. Res., Sect. A **506**, 250 (2003).
[34] K. X. Huang *et al.*, Nucl. Sci. Tech. **33**, 142 (2022).
[35] S. Jadach, B. F. L. Ward, and Z. Was, Phys. Rev. D **63**, 113009 (2001).
[36] S. Jadach, B. F. L. Ward, and Z. Was, Comput. Phys. Commun. **130**, 260 (2000).
[37] D. J. Lange, Nucl. Instrum. Methods Phys. Res., Sect. A **462**, 152 (2001).
[38] R. G. Ping, Chin. Phys. C **32**, 599 (2008).
[39] J. C. Chen, G. S. Huang, X. R. Qi, D. H. Zhang, and Y. S. Zhu, Phys. Rev. D **62**, 034003 (2000).
[40] R. L. Yang, R. G. Ping, and H. Chen, Chin. Phys. Lett. **31**, 061301 (2014).
[41] E. Barberio and Z. Was, Comput. Phys. Commun. **79**, 291 (1994).
[42] H. Albrecht *et al.* (ARGUS Collaboration), Phys. Lett. B **340**, 217 (1994).
[43] M. Ablikim *et al.* (BESIII Collaboration), Chin. Phys. C **36**, 915 (2012).
[44] N. Berger, B. Liu, and J. wang, J. Phys. Conf. Ser. **219**, 042031 (2010).
[45] B. S. Zou and D. V. Bugg, Eur. Phys. J. A **16**, 537 (2003).
[46] F. James and M. Roos, Comput. Phys. Commun. **10**, 343 (1975).
[47] See Supplemental Material at http://link.aps.org/supplemental/10.1103/PhysRevLett.134.191901, which includes Refs. [6,16,48,49], for additional information about PWA in the analysis.
[48] M. Ablikim *et al.* (BESIII Collaboration), Phys. Rev. Lett. **129**, 192002 (2022).
[49] M. Ablikim *et al.* (BESIII Collaboration), Phys. Rev. D **101**, 032008 (2020).
[50] M. Ablikim *et al.* (BESIII Collaboration), Phys. Rev. D **81**, 052005 (2010).
[51] M. Ablikim *et al.* (BESIII Collaboration), Phys. Rev. D **85**, 092012 (2012).

[52] M. Ablikim *et al.* (BESIII Collaboration), Phys. Rev. D **83**, 112005 (2011).
[53] M. Ablikim *et al.* (BESIII Collaboration), Phys. Rev. D **87**, 012002 (2013).
[54] F. von Hippel and C. Quigg, Phys. Rev. D **5**, 624 (1972).
[55] S. U. Chung, Phys. Rev. D **48**, 1225 (1993); **57**, 431 (1998).

M. Ablikim,[1] M. N. Achasov,[4,b] P. Adlarson,[75] O. Afedulidis,[3] X. C. Ai,[80] R. Aliberti,[35] A. Amoroso,[74a,74c] Q. An,[71,58]
Y. Bai,[57] O. Bakina,[36] I. Balossino,[29a] Y. Ban,[46,g] H.-R. Bao,[63] V. Batozskaya,[1,44] K. Begzsuren,[32] N. Berger,[35]
M. Berlowski,[44] M. Bertani,[28a] D. Bettoni,[29a] F. Bianchi,[74a,74c] E. Bianco,[74a,74c] A. Bortone,[74a,74c] I. Boyko,[36] R. A. Briere,[5]
A. Brueggemann,[68] H. Cai,[76] X. Cai,[1,58] A. Calcaterra,[28a] G. F. Cao,[1,63] N. Cao,[1,63] S. A. Cetin,[62a] J. F. Chang,[1,58]
W. L. Chang,[1,63] G. R. Che,[43] G. Chelkov,[36,a] C. Chen,[43] C. H. Chen,[9] Chao Chen,[55] G. Chen,[1] H. S. Chen,[1,63]
M. L. Chen,[1,58,63] S. J. Chen,[42] S. L. Chen,[45] S. M. Chen,[61] T. Chen,[1,63] X. R. Chen,[31,63] X. T. Chen,[1,63] Y. B. Chen,[1,58]
Y. Q. Chen,[34] Z. J. Chen,[25,h] Z. Y. Chen,[1,63] S. K. Choi,[10] X. Chu,[43] G. Cibinetto,[29a] F. Cossio,[74c] J. J. Cui,[50] H. L. Dai,[1,58]
J. P. Dai,[78] A. Dbeyssi,[18] R. E. de Boer,[3] D. Dedovich,[36] C. Q. Deng,[72] Z. Y. Deng,[1] A. Denig,[35] I. Denysenko,[36]
M. Destefanis,[74a,74c] F. De Mori,[74a,74c] B. Ding,[66,1] X. X. Ding,[46,g] Y. Ding,[34] Y. Ding,[40] J. Dong,[1,58] L. Y. Dong,[1,63]
M. Y. Dong,[1,58,63] X. Dong,[76] M. C. Du,[1] S. X. Du,[80] Z. H. Duan,[42] P. Egorov,[36,a] Y. H. Fan,[45] J. Fang,[1,58] J. Fang,[59]
S. S. Fang,[1,63] W. X. Fang,[1] Y. Fang,[1] Y. Q. Fang,[1,58] R. Farinelli,[29a] L. Fava,[74b,74c] F. Feldbauer,[3] G. Felici,[28a] C. Q. Feng,[71,58]
J. H. Feng,[59] Y. T. Feng,[71,58] K. Fischer,[69] M. Fritsch,[3] C. D. Fu,[1] J. L. Fu,[63] Y. W. Fu,[1] H. Gao,[63] Y. N. Gao,[46,g]
Yang Gao,[71,58] S. Garbolino,[74c] I. Garzia,[29a,29b] L. Ge,[80] P. T. Ge,[76] Z. W. Ge,[42] C. Geng,[59] E. M. Gersabeck,[67] A. Gilman,[69]
K. Goetzen,[13] L. Gong,[40] W. X. Gong,[1,58] W. Gradl,[35] S. Gramigna,[29a,29b] M. Greco,[74a,74c] M. H. Gu,[1,58] Y. T. Gu,[15]
C. Y. Guan,[1,63] Z. L. Guan,[22] A. Q. Guo,[31,63] L. B. Guo,[41] M. J. Guo,[50] R. P. Guo,[49] Y. P. Guo,[12,f] A. Guskov,[36,a]
J. Gutierrez,[27] K. L. Han,[63] T. T. Han,[1] X. Q. Hao,[19] F. A. Harris,[65] K. K. He,[55] K. L. He,[1,63] F. H. Heinsius,[3] C. H. Heinz,[35]
Y. K. Heng,[1,58,63] C. Herold,[60] T. Holtmann,[3] P. C. Hong,[12,f] G. Y. Hou,[1,63] X. T. Hou,[1,63] Y. R. Hou,[63] Z. L. Hou,[1] B. Y. Hu,[59]
H. M. Hu,[1,63] J. F. Hu,[56,i] T. Hu,[1,58,63] Y. Hu,[1] G. S. Huang,[71,58] K. X. Huang,[59] L. Q. Huang,[31,63] X. T. Huang,[50]
Y. P. Huang,[1] T. Hussain,[73] F. Hölzken,[3] N. Hüsken,[27,35] N. in der Wiesche,[68] M. Irshad,[71,58] J. Jackson,[27] S. Janchiv,[32]
J. H. Jeong,[10] Q. Ji,[1] Q. P. Ji,[19] W. Ji,[1,63] X. B. Ji,[1,63] X. L. Ji,[1,58] Y. Y. Ji,[50] X. Q. Jia,[50] Z. K. Jia,[71,58] D. Jiang,[1,63]
H. B. Jiang,[76] P. C. Jiang,[46,g] S. S. Jiang,[39] T. J. Jiang,[16] X. S. Jiang,[1,58,63] Y. Jiang,[63] J. B. Jiao,[50] J. K. Jiao,[34] Z. Jiao,[23]
S. Jin,[42] Y. Jin,[66] M. Q. Jing,[1,63] X. M. Jing,[63] T. Johansson,[75] S. Kabana,[33] N. Kalantar-Nayestanaki,[64] X. L. Kang,[9]
X. S. Kang,[40] M. Kavatsyuk,[64] B. C. Ke,[80] V. Khachatryan,[27] A. Khoukaz,[68] R. Kiuchi,[1] O. B. Kolcu,[62a] B. Kopf,[3]
M. Kuessner,[3] X. Kui,[1,63] N. Kumar,[26] A. Kupsc,[44,75] W. Kühn,[37] J. J. Lane,[67] P. Larin,[18] L. Lavezzi,[74a,74c] T. T. Lei,[71,58]
Z. H. Lei,[71,58] H. Leithoff,[35] M. Lellmann,[35] T. Lenz,[35] C. Li,[47] C. Li,[43] C. H. Li,[39] Cheng Li,[71,58] D. M. Li,[80] F. Li,[1,58] G. Li,[1]
H. Li,[71,58] H. B. Li,[1,63] H. J. Li,[19] H. N. Li,[56,i] Hui Li,[43] J. R. Li,[61] J. S. Li,[59] Ke Li,[1] L. J. Li,[1,63] L. K. Li,[1] Lei Li,[48] M. H. Li,[43]
P. R. Li,[38,k] Q. M. Li,[1,63] Q. X. Li,[50] R. Li,[17,31] S. X. Li,[12] T. Li,[50] W. D. Li,[1,63] W. G. Li,[1] X. Li,[1,63] X. H. Li,[71,58] X. L. Li,[50]
Xiaoyu Li,[1,63] Y. G. Li,[46,g] Z. J. Li,[59] Z. X. Li,[15] C. Liang,[42] H. Liang,[71,58] H. Liang,[1,63] Y. F. Liang,[54] Y. T. Liang,[31,63]
G. R. Liao,[14] L. Z. Liao,[50] Y. P. Liao,[1,63] J. Libby,[26] A. Limphirat,[60] D. X. Lin,[31,63] T. Lin,[1] B. J. Liu,[1] B. X. Liu,[76] C. Liu,[34]
C. X. Liu,[1] F. H. Liu,[53] Fang Liu,[1] Feng Liu,[6] G. M. Liu,[56,i] H. Liu,[38,j,k] H. B. Liu,[15] H. M. Liu,[1,63] Huanhuan Liu,[1]
Huihui Liu,[21] J. B. Liu,[71,58] J. Y. Liu,[1,63] K. Liu,[38,j,k] K. Y. Liu,[40] Ke Liu,[22] L. Liu,[71,58] L. C. Liu,[43] Lu Liu,[43] M. H. Liu,[12,f]
P. L. Liu,[1] Q. Liu,[63] S. B. Liu,[71,58] T. Liu,[12,f] W. K. Liu,[43] W. M. Liu,[71,58] X. Liu,[38,j,k] X. Liu,[39] Y. Liu,[38,j,k] Y. Liu,[80]
Y. B. Liu,[43] Z. A. Liu,[1,58,63] Z. D. Liu,[9] Z. Q. Liu,[50] X. C. Lou,[1,58,63] F. X. Lu,[59] H. J. Lu,[23] J. G. Lu,[1,58] X. L. Lu,[1] Y. Lu,[7]
Y. P. Lu,[1,58] Z. H. Lu,[1,63] C. L. Luo,[41] M. X. Luo,[79] T. Luo,[12,f] X. L. Luo,[1,58] X. R. Lyu,[63] Y. F. Lyu,[43] F. C. Ma,[40] H. Ma,[78]
H. L. Ma,[1] J. L. Ma,[1,63] L. L. Ma,[50] M. M. Ma,[1,63] Q. M. Ma,[1] R. Q. Ma,[1,63] X. T. Ma,[1,63] X. Y. Ma,[1,58] Y. Ma,[46,g] Y. M. Ma,[31]
F. E. Maas,[18] M. Maggiora,[74a,74c] S. Malde,[69] A. Mangoni,[28b] Y. J. Mao,[46,g] Z. P. Mao,[1] S. Marcello,[74a,74c] Z. X. Meng,[66]
J. G. Messchendorp,[13,64] G. Mezzadri,[29a] H. Miao,[1,63] T. J. Min,[42] R. E. Mitchell,[27] X. H. Mo,[1,58,63] B. Moses,[27]
N. Yu. Muchnoi,[4,b] J. Muskalla,[35] Y. Nefedov,[36] F. Nerling,[18,d] I. B. Nikolaev,[4,b] Z. Ning,[1,58] S. Nisar,[11,l] Q. L. Niu,[38,j,k]
W. D. Niu,[55] Y. Niu,[50] S. L. Olsen,[63] Q. Ouyang,[1,58,63] S. Pacetti,[28b,28c] X. Pan,[55] Y. Pan,[57] A. Pathak,[34] P. Patteri,[28a]
Y. P. Pei,[71,58] M. Pelizaeus,[3] H. P. Peng,[71,58] Y. Y. Peng,[38,j,k] K. Peters,[13,d] J. L. Ping,[41] R. G. Ping,[1,63] S. Plura,[35] V. Prasad,[33]
F. Z. Qi,[1] H. Qi,[71,58] H. R. Qi,[61] M. Qi,[42] T. Y. Qi,[12,f] S. Qian,[1,58] W. B. Qian,[63] C. F. Qiao,[63] X. K. Qiao,[80] J. J. Qin,[72]
L. Q. Qin,[14] X. S. Qin,[50] Z. H. Qin,[1,58] J. F. Qiu,[1] S. Q. Qu,[61] Z. H. Qu,[72] C. F. Redmer,[35] K. J. Ren,[39] A. Rivetti,[74c]

M. Rolo,[74c] G. Rong,[1,63] Ch. Rosner,[18] S. N. Ruan,[43] N. Salone,[44] A. Sarantsev,[36,c] Y. Schelhaas,[35] K. Schoenning,[75]
M. Scodeggio,[29a] K. Y. Shan,[12,f] W. Shan,[24] X. Y. Shan,[71,58] Z. J. Shang,[38,j,k] J. F. Shangguan,[55] L. G. Shao,[1,63] M. Shao,[71,58]
C. P. Shen,[12,f] H. F. Shen,[1,8] W. H. Shen,[63] X. Y. Shen,[1,63] B. A. Shi,[63] H. C. Shi,[71,58] J. L. Shi,[12] J. Y. Shi,[1] Q. Q. Shi,[55]
R. S. Shi,[1,63] S. Y. Shi,[72] X. Shi,[1,58] J. J. Song,[19] T. Z. Song,[59] W. M. Song,[34,1] Y. J. Song,[12] Y. X. Song,[46,g,m] S. Sosio,[74a,74c]
S. Spataro,[74a,74c] F. Stieler,[35] Y. J. Su,[63] G. B. Sun,[76] G. X. Sun,[1] H. Sun,[63] H. K. Sun,[1] J. F. Sun,[19] K. Sun,[61] L. Sun,[76]
S. S. Sun,[1,63] T. Sun,[51,e] W. Y. Sun,[34] Y. Sun,[9] Y. J. Sun,[71,58] Y. Z. Sun,[1] Z. Q. Sun,[1,63] Z. T. Sun,[50] C. J. Tang,[54] G. Y. Tang,[1]
J. Tang,[59] Y. A. Tang,[76] L. Y. Tao,[72] Q. T. Tao,[25,h] M. Tat,[69] J. X. Teng,[71,58] V. Thoren,[75] W. H. Tian,[59] Y. Tian,[31,63]
Z. F. Tian,[76] I. Uman,[62b] Y. Wan,[55] S. J. Wang,[50] B. Wang,[1] B. L. Wang,[63] Bo Wang,[71,58] D. Y. Wang,[46,g] F. Wang,[72]
H. J. Wang,[38,j,k] J. P. Wang,[50] K. Wang,[1,58] L. L. Wang,[1] M. Wang,[50] Meng Wang,[1,63] N. Y. Wang,[63] S. Wang,[38,j,k]
S. Wang,[12,f] T. Wang,[12,f] T. J. Wang,[43] W. Wang,[59] W. Wang,[72] W. P. Wang,[71,58] X. Wang,[46,g] X. F. Wang,[38,j,k] X. J. Wang,[39]
X. L. Wang,[12,f] X. N. Wang,[1] Y. Wang,[61] Y. D. Wang,[45] Y. F. Wang,[1,58,63] Y. L. Wang,[19] Y. N. Wang,[45] Y. Q. Wang,[1]
Yaqian Wang,[17] Yi Wang,[61] Z. Wang,[1,58] Z. L. Wang,[72] Z. Y. Wang,[1,63] Ziyi Wang,[63] D. Wei,[70] D. H. Wei,[14] F. Weidner,[68]
S. P. Wen,[1] Y. R. Wen,[39] U. Wiedner,[3] G. Wilkinson,[69] M. Wolke,[75] L. Wollenberg,[3] C. Wu,[39] J. F. Wu,[1,8] L. H. Wu,[1]
L. J. Wu,[1,63] X. Wu,[12,f] X. H. Wu,[34] Y. Wu,[71] Y. H. Wu,[55] Y. J. Wu,[31] Z. Wu,[1,58] L. Xia,[71,58] X. M. Xian,[39] B. H. Xiang,[1,63]
T. Xiang,[46,g] D. Xiao,[38,j,k] G. Y. Xiao,[42] S. Y. Xiao,[1] Y. L. Xiao,[12,f] Z. J. Xiao,[41] C. Xie,[42] X. H. Xie,[46,g] Y. Xie,[50]
Y. G. Xie,[1,58] Y. H. Xie,[6] Z. P. Xie,[71,58] T. Y. Xing,[1,63] C. F. Xu,[1,63] C. J. Xu,[59] G. F. Xu,[1] H. Y. Xu,[66] Q. J. Xu,[16] Q. N. Xu,[30]
W. Xu,[1] W. L. Xu,[66] X. P. Xu,[55] Y. C. Xu,[77] Z. P. Xu,[42] Z. S. Xu,[63] F. Yan,[12,f] L. Yan,[12,f] W. B. Yan,[71,58] W. C. Yan,[80]
X. Q. Yan,[1] H. J. Yang,[51,e] H. L. Yang,[34] H. X. Yang,[1] Tao Yang,[1] Y. Yang,[12,f] Y. F. Yang,[43] Y. X. Yang,[1,63] Yifan Yang,[1,63]
Z. W. Yang,[38,j,k] Z. P. Yao,[50] M. Ye,[1,58] M. H. Ye,[8] J. H. Yin,[1] Z. Y. You,[59] B. X. Yu,[1,58,63] C. X. Yu,[43] G. Yu,[1,63] J. S. Yu,[25,h]
T. Yu,[72] X. D. Yu,[46,g] Y. C. Yu,[80] C. Z. Yuan,[1,63] J. Yuan,[34] L. Yuan,[2] S. C. Yuan,[1] Y. Yuan,[1,63] Z. Y. Yuan,[59] C. X. Yue,[39]
A. A. Zafar,[73] F. R. Zeng,[50] S. H. Zeng,[72] X. Zeng,[12,f] Y. Zeng,[25,h] Y. J. Zeng,[59] Y. J. Zeng,[1,63] X. Y. Zhai,[34] Y. C. Zhai,[50]
Y. H. Zhan,[59] A. Q. Zhang,[1,63] B. L. Zhang,[1,63] B. X. Zhang,[1] D. H. Zhang,[43] G. Y. Zhang,[19] H. Zhang,[71] H. C. Zhang,[1,58,63]
H. H. Zhang,[59] H. H. Zhang,[34] H. Q. Zhang,[1,58,63] H. Y. Zhang,[1,58] J. Zhang,[80] J. Zhang,[59] J. J. Zhang,[52] J. L. Zhang,[20]
J. Q. Zhang,[41] J. W. Zhang,[1,58,63] J. X. Zhang,[38,j,k] J. Y. Zhang,[1] J. Z. Zhang,[1,63] Jianyu Zhang,[63] L. M. Zhang,[61] Lei Zhang,[42]
P. Zhang,[1,63] Q. Y. Zhang,[39,80] R. Y. Zhang,[38,j,k] Shuihan Zhang,[1,63] Shulei Zhang,[25,h] X. D. Zhang,[45] X. M. Zhang,[1]
X. Y. Zhang,[50] Y. Zhang,[72] Y. T. Zhang,[80] Y. H. Zhang,[1,58] Y. M. Zhang,[39] Yan Zhang,[71,58] Yao Zhang,[1] Z. D. Zhang,[1]
Z. H. Zhang,[1] Z. L. Zhang,[34] Z. Y. Zhang,[76] Z. Y. Zhang,[43] G. Zhao,[1] J. Y. Zhao,[1,63] J. Z. Zhao,[1,58] Lei Zhao,[71,58] Ling Zhao,[1]
M. G. Zhao,[43] R. P. Zhao,[63] S. J. Zhao,[80] Y. B. Zhao,[1,58] Y. X. Zhao,[31,63] Z. G. Zhao,[71,58] A. Zhemchugov,[36,a] B. Zheng,[72]
J. P. Zheng,[1,58] W. J. Zheng,[1,63] Y. H. Zheng,[63] B. Zhong,[41] X. Zhong,[59] H. Zhou,[50] J. Y. Zhou,[34] L. P. Zhou,[1,63] X. Zhou,[76]
X. K. Zhou,[6] X. R. Zhou,[71,58] X. Y. Zhou,[39] Y. Z. Zhou,[12,f] J. Zhu,[43] K. Zhu,[1] K. J. Zhu,[1,58,63] L. Zhu,[34] L. X. Zhu,[63]
S. H. Zhu,[70] S. Q. Zhu,[42] T. J. Zhu,[12,f] W. J. Zhu,[12,f] Y. C. Zhu,[71,58] Z. A. Zhu,[1,63] J. H. Zou,[1] and J. Zu[71,58]

(BESIII Collaboration)

[1]*Institute of High Energy Physics, Beijing 100049, People's Republic of China*
[2]*Beihang University, Beijing 100191, People's Republic of China*
[3]*Bochum Ruhr-University, D-44780 Bochum, Germany*
[4]*Budker Institute of Nuclear Physics SB RAS (BINP), Novosibirsk 630090, Russia*
[5]*Carnegie Mellon University, Pittsburgh, Pennsylvania 15213, USA*
[6]*Central China Normal University, Wuhan 430079, People's Republic of China*
[7]*Central South University, Changsha 410083, People's Republic of China*
[8]*China Center of Advanced Science and Technology, Beijing 100190, People's Republic of China*
[9]*China University of Geosciences, Wuhan 430074, People's Republic of China*
[10]*Chung-Ang University, Seoul, 06974, Republic of Korea*
[11]*COMSATS University Islamabad, Lahore Campus, Defence Road, Off Raiwind Road, 54000 Lahore, Pakistan*
[12]*Fudan University, Shanghai 200433, People's Republic of China*
[13]*GSI Helmholtzcentre for Heavy Ion Research GmbH, D-64291 Darmstadt, Germany*
[14]*Guangxi Normal University, Guilin 541004, People's Republic of China*
[15]*Guangxi University, Nanning 530004, People's Republic of China*
[16]*Hangzhou Normal University, Hangzhou 310036, People's Republic of China*
[17]*Hebei University, Baoding 071002, People's Republic of China*

[18]Helmholtz Institute Mainz, Staudinger Weg 18, D-55099 Mainz, Germany
[19]Henan Normal University, Xinxiang 453007, People's Republic of China
[20]Henan University, Kaifeng 475004, People's Republic of China
[21]Henan University of Science and Technology, Luoyang 471003, People's Republic of China
[22]Henan University of Technology, Zhengzhou 450001, People's Republic of China
[23]Huangshan College, Huangshan 245000, People's Republic of China
[24]Hunan Normal University, Changsha 410081, People's Republic of China
[25]Hunan University, Changsha 410082, People's Republic of China
[26]Indian Institute of Technology Madras, Chennai 600036, India
[27]Indiana University, Bloomington, Indiana 47405, USA
[28a]INFN Laboratori Nazionali di Frascati, INFN Laboratori Nazionali di Frascati, I-00044, Frascati, Italy
[28b]INFN Sezione di Perugia, I-06100, Perugia, Italy
[28c]University of Perugia, I-06100, Perugia, Italy
[29a]INFN Sezione di Ferrara, INFN Sezione di Ferrara, I-44122, Ferrara, Italy
[29b]University of Ferrara, I-44122, Ferrara, Italy
[30]Inner Mongolia University, Hohhot 010021, People's Republic of China
[31]Institute of Modern Physics, Lanzhou 730000, People's Republic of China
[32]Institute of Physics and Technology, Peace Avenue 54B, Ulaanbaatar 13330, Mongolia
[33]Instituto de Alta Investigación, Universidad de Tarapacá, Casilla 7D, Arica 1000000, Chile
[34]Jilin University, Changchun 130012, People's Republic of China
[35]Johannes Gutenberg University of Mainz, Johann-Joachim-Becher-Weg 45, D-55099 Mainz, Germany
[36]Joint Institute for Nuclear Research, 141980 Dubna, Moscow region, Russia
[37]Justus-Liebig-Universitaet Giessen, II. Physikalisches Institut, Heinrich-Buff-Ring 16, D-35392 Giessen, Germany
[38]Lanzhou University, Lanzhou 730000, People's Republic of China
[39]Liaoning Normal University, Dalian 116029, People's Republic of China
[40]Liaoning University, Shenyang 110036, People's Republic of China
[41]Nanjing Normal University, Nanjing 210023, People's Republic of China
[42]Nanjing University, Nanjing 210093, People's Republic of China
[43]Nankai University, Tianjin 300071, People's Republic of China
[44]National Centre for Nuclear Research, Warsaw 02-093, Poland
[45]North China Electric Power University, Beijing 102206, People's Republic of China
[46]Peking University, Beijing 100871, People's Republic of China
[47]Qufu Normal University, Qufu 273165, People's Republic of China
[48]Renmin University of China, Beijing 100872, People's Republic of China
[49]Shandong Normal University, Jinan 250014, People's Republic of China
[50]Shandong University, Jinan 250100, People's Republic of China
[51]Shanghai Jiao Tong University, Shanghai 200240, People's Republic of China
[52]Shanxi Normal University, Linfen 041004, People's Republic of China
[53]Shanxi University, Taiyuan 030006, People's Republic of China
[54]Sichuan University, Chengdu 610064, People's Republic of China
[55]Soochow University, Suzhou 215006, People's Republic of China
[56]South China Normal University, Guangzhou 510006, People's Republic of China
[57]Southeast University, Nanjing 211100, People's Republic of China
[58]State Key Laboratory of Particle Detection and Electronics, Beijing 100049, Hefei 230026, People's Republic of China
[59]Sun Yat-Sen University, Guangzhou 510275, People's Republic of China
[60]Suranaree University of Technology, University Avenue 111, Nakhon Ratchasima 30000, Thailand
[61]Tsinghua University, Beijing 100084, People's Republic of China
[62a]Turkish Accelerator Center Particle Factory Group, Istinye University, 34010, Istanbul, Turkey
[62b]Near East University, Nicosia, North Cyprus, 99138, Mersin 10, Turkey
[63]University of Chinese Academy of Sciences, Beijing 100049, People's Republic of China
[64]University of Groningen, NL-9747 AA Groningen, The Netherlands
[65]University of Hawaii, Honolulu, Hawaii 96822, USA
[66]University of Jinan, Jinan 250022, People's Republic of China
[67]University of Manchester, Oxford Road, Manchester, M13 9PL, United Kingdom
[68]University of Muenster, Wilhelm-Klemm-Strasse 9, 48149 Muenster, Germany
[69]University of Oxford, Keble Road, Oxford OX13RH, United Kingdom
[70]University of Science and Technology Liaoning, Anshan 114051, People's Republic of China
[71]University of Science and Technology of China, Hefei 230026, People's Republic of China
[72]University of South China, Hengyang 421001, People's Republic of China
[73]University of the Punjab, Lahore-54590, Pakistan

[74a]*University of Turin and INFN, University of Turin, I-10125, Turin, Italy*
[74b]*University of Eastern Piedmont, I-15121, Alessandria, Italy*
[74c]*INFN, I-10125, Turin, Italy*
[75]*Uppsala University, Box 516, SE-75120 Uppsala, Sweden*
[76]*Wuhan University, Wuhan 430072, People's Republic of China*
[77]*Yantai University, Yantai 264005, People's Republic of China*
[78]*Yunnan University, Kunming 650500, People's Republic of China*
[79]*Zhejiang University, Hangzhou 310027, People's Republic of China*
[80]*Zhengzhou University, Zhengzhou 450001, People's Republic of China*

[a] Also at the Moscow Institute of Physics and Technology, Moscow 141700, Russia.
[b] Also at the Novosibirsk State University, Novosibirsk, 630090, Russia.
[c] Also at the NRC "Kurchatov Institute", PNPI, 188300, Gatchina, Russia.
[d] Also at Goethe University Frankfurt, 60323 Frankfurt am Main, Germany.
[e] Also at Key Laboratory for Particle Physics, Astrophysics and Cosmology, Ministry of Education; Shanghai Key Laboratory for Particle Physics and Cosmology; Institute of Nuclear and Particle Physics, Shanghai 200240, People's Republic of China.
[f] Also at Key Laboratory of Nuclear Physics and Ion-beam Application (MOE) and Institute of Modern Physics, Fudan University, Shanghai 200443, People's Republic of China.
[g] Also at State Key Laboratory of Nuclear Physics and Technology, Peking University, Beijing 100871, People's Republic of China.
[h] Also at School of Physics and Electronics, Hunan University, Changsha 410082, People's Republic of China.
[i] Also at Guangdong Provincial Key Laboratory of Nuclear Science, Institute of Quantum Matter, South China Normal University, Guangzhou 510006, People's Republic of China.
[j] Also at MOE Frontiers Science Center for Rare Isotopes, Lanzhou University, Lanzhou 730000, People's Republic of China.
[k] Also at Lanzhou Center for Theoretical Physics, Lanzhou University, Lanzhou 730000, People's Republic of China.
[l] Also at the Department of Mathematical Sciences, IBA, Karachi 75270, Pakistan.
[m] Also at Ecole Polytechnique Federale de Lausanne (EPFL), CH-1015 Lausanne, Switzerland.